PHYSICAL REVIEW B, VOLUME 65, 014111

Polarization properties of ZnO and BeO: An *ab initio* study through the Berry phase and Wannier functions approaches

Y. Noel,[1] C. M. Zicovich-Wilson,[2,*] B. Civalleri,[2] Ph. D'Arco,[1] and R. Dovesi[2,3,†]
[1]*Laboratoire PMMP, Université Pierre et Marie Curie, Paris 6, 4 Place Jussieu, 75252 Paris Cedex 05, France*
[2]*Department CIFM, University of Torino, via Giuria 5, I-10125 Torino, Italy*
[3]*Unità INFM di Torino, Sezione F, via Giuria 5, I-10125 Torino, Italy*
(Received 5 June 2001; published 12 December 2001)

The spontaneous polarization and the piezoelectric constants of ZnO and BeO are calculated at an *ab initio* quantum-mechanical level by using two alternative strategies, namely, through the Berry phase scheme applied to delocalized crystalline orbitals, and through the definition of well-localized Wannier functions. The two sets of results, obtained in the same computational conditions (both schemes are implemented in the CRYSTAL code) compare extremely well, and are in good agreement with available experimental data.

DOI: 10.1103/PhysRevB.65.014111 PACS number(s): 71.23.An, 71.15.−m, 77.65.−j

I. INTRODUCTION

The crystalline orbitals (CO's) describing the electronic ground state of a periodic system are usually obtained as a linear combination of (delocalized) Bloch functions (BF's), in order to exploit the block factorization of the Hamiltonian matrix, because BF's are bases of the irreducible representations of the translation group. Localized Wannier functions (LWF's) can be obtained by applying a unitary transformation to these CO's; well-localized WF's present many interesting features, because of the following reasons (see, for example, the conclusions section in Ref. 1).

(i) LWF's permit an easy and intuitive description of the electronic structure of crystalline compounds in terms of chemical concepts, such as lone pairs, shared electrons, covalent or ionic bonds.[2–8]

(ii) Localized orbitals have been used for the implementation of *post* Hartree-Fock estimates of correlation energy in large molecules, using the methods either of many-body perturbation[9–14] or configuration-interaction and coupled-cluster[15–21] theories. These methods can be straightforwardly extended to periodic systems through the definition of a set of well-localized WF's.

(iii) Many properties can be evaluated in an extremely simple and intuitive way when starting from LWF's, whereas expensive and not easy to implement methods are required, when delocalized CO's are used. This is the case, for example, of the polarization (**P**) (and the effective Born charges Z^*),[22,23] which in the localized representation is nothing else but the difference in the dipole moment of the cell-charge distributions evaluated at two different geometries (see below for a more precise definition), whereas in the BF representation it is evaluated through a formalism based on Berry phases (BP's),[24–27] which requires the evaluation of relatively complicated integrals.

In the present paper we compute the piezoelectric tensor of ZnO and BeO and the various contributions to it by starting from LWF's; they are in turn obtained from the CO's represented in a basis of BF's through a localization scheme recently implemented by us.[28] The piezoelectric-tensor components take a very simple form in the WF basis, as they are related to the dependence of the centroids of WF's on the applied strain. The same quantities (as a by product, we will obtain also the spontaneous polarization **P** and the transverse Born charges Z^*) will also be computed through the BP technique, already implemented in the CRYSTAL code.[29]

II. METHODOLOGICAL ASPECT

A. Computational details

Calculations have been performed at the Hartree-Fock (HF) level with the periodic *ab initio* CRYSTAL program.[30] In CRYSTAL, BF's are built from localized functions, to be indicated in the following as atomic orbitals (AO's), which are contractions (linear combinations with fixed coefficients) of Gaussian-type functions (GTF's). A GTF is the product of a Gaussian times a real solid spherical harmonic.

An all-electron basis set has been used. It is the same as in Refs. 31–33. For Zn, Be, and O an 86-4111(41)G, 5-11G, and 8-411(1)G contraction has been adopted, where the first number refers to an s shell, the others are sp shells; d shell contractions are given in parentheses. The exponents of the two most diffuse sp and of the d shells of the oxygen atom are 0.48, 0.20, and 0.65 (ZnO) and 0.47, 0.18, and 0.60 bohr^{-2} (BeO). As regards the computational conditions, standard values of the tolerances as defined in the CRYSTAL manual[30] have been adopted. Both systems have the wurtzite structure, and the calculated equilibrium-geometry parameters are given in Table I.

B. The localized Wannier functions scheme and the piezoelectricity calculations

1. The localized Wannier functions scheme

In the following, the most relevant features of the method employed to obtain LWF's are briefly described. A more detailed discussion on the various aspects of the scheme is reported elsewhere.[28] In the present periodic calculations BF's, $\psi_t(\mathbf{k})$, are given in terms of the basis set of AO's, $\{\varphi_\mu(\mathbf{r}-\mathbf{s}_\mu-\mathbf{g})\}$, as

TABLE I. Calculated and experimental cell parameters for BeO and ZnO. a_0 and c_0 in Å; u_0 and $u_0-0.5$ are the fractional coordinates of the oxygen atoms along the c axis.

		a_0	c_0	c_0/a_0	u_0
BeO	Our work	2.688	4.351	1.619	0.379
	Expt.	2.698	4.376	1.622	0.378
ZnO	Our work	3.281	5.250	1.600	0.383
	Expt.	3.250	5.21	1.602	0.382

[a] Reference 42.

[b] Reference 43.

$$\psi_t(\mathbf{r},\mathbf{k})=\sum_{\mu=1}^{M}\alpha_{\mu t}(\mathbf{k})\sum_{\mathbf{g}}e^{i\mathbf{k}\cdot\mathbf{g}}\varphi_\mu(\mathbf{r}-\mathbf{s}_\mu-\mathbf{g}), \tag{1}$$

where $\mathbf{k}$ is a reciprocal lattice vector within the first Brillouin zone (BZ), and the first and second sums in the right-hand side run over the AO's in the cell and the lattice cells, respectively. Given the set $\{\psi_t(\mathbf{k}),\ \forall\ \mathbf{k}\in\mathrm{BZ}\}$ of band t, the tth reference WF (a WF conventionally assigned to the reference cell) is given in the AO basis set as

$$\omega_t(\mathbf{r})=\sum_{\mu=1}^{M}\sum_{\mathbf{g}}c^{\mathbf{g}}_{\mu t}\varphi_\mu(\mathbf{r}-\mathbf{s}_\mu-\mathbf{g}), \tag{2}$$

where the orthonormality condition $\langle\omega^{\mathbf{g}}_t|\omega^{\mathbf{g}'}_t\rangle=\delta'_{\mathbf{gg}}$ holds for the periodic images $|\omega^{\mathbf{g}}_t\rangle\equiv\omega_t(\mathbf{r}-\mathbf{g})$ of $|\omega_t\rangle\equiv|\omega^{\mathbf{0}}_t\rangle$. In addition, coefficients $\alpha_{\mu t}(\mathbf{k})$ and $c^{\mathbf{g}}_{\mu t}$ in Eqs. (1) and (2), respectively, are related by Fourier-like transforms,

$$c^{\mathbf{g}}_{\mu t}=\frac{V}{(2\pi)^3}\int_{\mathrm{BZ}}d\mathbf{k}\,e^{i\mathbf{k}\cdot\mathbf{g}}\alpha_{\mu t}(\mathbf{k})=\frac{1}{L}\sum_{j=0}^{L-1}e^{i\mathbf{k}_j\cdot\mathbf{g}}\alpha_{\mu t}(\mathbf{k}_j), \tag{3}$$

$$\alpha_{\mu t}(\mathbf{k})=\sum_{\mathbf{g}}e^{-i\mathbf{k}\cdot\mathbf{g}}c^{\mathbf{g}}_{\mu t}. \tag{4}$$

In the first equality of Eq. (3), integration is performed over the BZ and V is the cell volume, while in the second equality the finite approach is used and $\mathbf{k}_j$ are the nodes of a Monkhorst-Pack net within the BZ.[34] In Eq. (3), it is assumed that the Γ point always belongs to the net and is labeled as $\mathbf{k}_0$. Within this approach the number of nodes L is the same as the number of effective cells that are to be considered in the corresponding sums of Eqs. (1), (2), and (4).

Starting from a set of N bands given in terms of BF's $\{\psi_t(\mathbf{k}_j)\}_{t=1}^{N}$, where $j=1,\ldots,L$, the present method provides a set of LWF's that spans the same subspace as the original BF's. The method is based on the iterative application of a Wannierization step, which yields a set of WF's as similar as possible (under a suitable criterion) to a given set of spatially localized model functions $\mathcal{F}_t$ (not necessarily WF's), and a Boys-like localization[35,36] performed only within the subspace spanned by the reference WF's given in the form of Eq. (2). Model functions $\mathcal{F}_t$ employed in the Wannierization step are obtained from the Boys-localized WF's of the previous cycle by means of

$$\mathcal{F}_t(\mathbf{r})=\sum_{A=1}^{P}p_{A,t}\sum_{\mu\in A}c^{\mathbf{G}_{A,t}}_{\mu t}\varphi_\mu(\mathbf{r}-\mathbf{s}_\mu-\mathbf{G}_{A,t}), \tag{5}$$

where $c^{\mathbf{g}}_{\mu t}$ are the coefficients of the tth WF's, the first and second sums run over the P atoms in the cell and the AO's in atom A, respectively. Concerning matrices $\mathbf{G}_{A,t}$ and $p_{A,t}$, they are used in Eq. (5) just to select the most relevant AO coefficients of the original WF's in the construction of functions $\mathcal{F}_t$. In this way, the localized character of the model functions is always improved with respect to the original ones.[28] The criteria employed to define matrices $\mathbf{G}_{A,t}$ and $p_{A,t}$ are based on the atomic populations of WF t, $q^{\mathbf{g}}_{A,t}$, which are obtained by means of the well-known Mulliken partition of the electronic density as

$$q^{\mathbf{g}}_{A,t}=\sum_{\mu\in A}\sum_{\nu,\mathbf{g}'}c^{\mathbf{g}}_{\mu t}c^{\mathbf{g}+\mathbf{g}'}_{\nu t}S^{\mathbf{g}'}_{\mu\nu}, \tag{6}$$

where $S^{\mathbf{g}'}_{\mu\nu}=\langle\varphi^{\mathbf{0}}_\mu|\varphi^{\mathbf{g}'}_\nu\rangle$ is the overlap matrix in the AO basis set. Accordingly, $\mathbf{G}_{A,t}$ is the cell where is situated the periodic image of atom A that displays the maximum atomic population, $q^{\mathbf{g}}_{A,t}$, in WF t. On the other hand, given a predefined threshold θ, factors $p_{A,t}$ read

$$p_{A,t}=\begin{cases}0 & \text{if } q^{\mathbf{g}}_{A,t}<\theta\quad\forall\ \mathbf{g}\\ 1 & \text{otherwise}\end{cases}. \tag{7}$$

It is worth noting that Eq. (7) guarantees that only contributions coming from atoms whose atomic population is greater than θ are actually considered in Eq. (5). This is used to correct the troubles in the convergence of the iterative process caused by the numerical indetermination of the WF tails in the first stages of the calculation.[28]

In the Wannierization step, functions $\mathcal{F}_t$ are transformed into a set of nonorthonormal BF's according to Eq. (4), then projected onto the chosen subspace using operators $Q(\mathbf{k}_j)=\sum_{t=1}^{N}|\psi_t(\mathbf{k}_j)\rangle\langle\psi_t(\mathbf{k}_j)|$, and next, symmetrically orthonormalized. The resulting BF's are back-transformed into WF's employing Eq. (3). These WF's are the inputs of the subsequent Boys-localization step and a new cycle starts.

At the end of each cycle the overall delocalization index Λ is calculated as

$$\Lambda=\left[\frac{1}{N}\sum_{t=1}^{N}\sum_{A,\mathbf{g}}(q^{\mathbf{g}}_{A,t})^2\right]^{-1}, \tag{8}$$

and the iterative process stops when the absolute difference in Λ between two consecutive cycles is less than a given threshold. The parameters used to control the accuracy and efficiency of the various steps of the localization process are the same as previously reported.[28,37]

The degree of localization of the LWF t is here measured in terms of two indices, namely, λ_t and σ_t, given by the following expressions:

$$\lambda_t = \left[\sum_{A,\mathbf{g}} (q_{A,t}^{\mathbf{g}})^2 \right]^{-1}, \tag{9}$$

$$\sigma_t = \langle \omega_t | (\mathbf{r} - \overline{\mathbf{r}}_t)^2 | \omega_t \rangle^{1/2}, \tag{10}$$

where

$$\overline{\mathbf{r}}_t = \int d\mathbf{r}\, \mathbf{r} |\omega_t|^2 \tag{11}$$

is the centroid of the tth LWF. It is to be noted that λ_t is nothing other than an inverse participation ratio of the atomic populations of WF t.

TABLE II. Characterization of the WF's of ZnO and BeO. λ is the localization index [see Eq. (9)], d is the distance of the WF centroid $\overline{\mathbf{r}}$ from the nearest atom (third column), σ is given by Eq. (10). N_{WF} is the number of equivalent WF (that is, with the same value of λ, d, and σ, and centered on the same atom).

System	Atom (type)	N_{WF}	λ	d(Å)	σ (Å)
ZnO	Zn	5	1.006	0.011	0.527
	O (1)	3	1.163	0.368	0.800
	O (2)	1	1.161	0.366	0.801
BeO	O (1)	3	1.033	0.369	0.745
	O (2)	1	1.031	0.370	0.747

2. Spontaneous polarization and piezoelectricity through the LWF scheme.

In terms of the LWF, the electronic contribution to the spontaneous polarization $\mathbf{P}_{el}$ takes a very simple form,

$$\mathbf{P}_{el} = \frac{-2e}{V} \sum_{t=1}^{N} (\overline{\mathbf{r}}_t^{(1)} - \overline{\mathbf{r}}_t^{(0)}), \tag{12}$$

where $\overline{\mathbf{r}}_t^{(\xi)}$ is the centroid of the tth LWF [Eq. (11)] in the (ξ) nuclear and cell configuration. The nuclear contribution takes a form very similar to Eq. (12),

$$\mathbf{P}_{nuc} = \frac{e}{V} \sum_{A=1}^{P} (\mathbf{r}_A^{(1)} - \mathbf{r}_A^{(0)}) Z_A, \tag{13}$$

where $\mathbf{r}_A^{(\xi)}$ is the position of nucleus A in configuration (ξ) and Z_A is its atomic number. It is clear that both terms, Eqs. (12) and (13) as well as their sum $\mathbf{P}$ are defined modulo (e/V) $\mathbf{R}$, where $\mathbf{R}$ is any direct-lattice-translation vector, so that, in principle, many (infinite) values of $\mathbf{P}$ [each one defines a branch (b) of a multivaluated function] are obtained, $\mathbf{P}^{(b')} = \mathbf{P}^{(b)} + (e/V)\mathbf{R}$, and one should decide which branch is the "good one." This is not a difficulty in practice for the calculation of the spontaneous polarization $\mathbf{P}_{eq}$, because in most cases the smallest possible value $\mathbf{P}_{eq}^{(m)}$ is such that $|\mathbf{P}_{eq}^{(m)}| \ll |(e/V)\mathbf{R}|\ \forall\ \ \mathbf{R}$, and is much closer to the experimental value than any other determination, so that this choice can be assumed as a rule for all cases.[38] The situation is slightly more complicated when derivatives are involved, as is the case of the piezoelectric constants e_{ij}. The latter are defined through the relation (valid in the linear regime)

$$P_i = \sum_j e_{ij} \varepsilon_j, \tag{14}$$

where ε_j is the strain tensor component (Voigt's notation has been used). e_{ij} is then obtained as follows:

$$e_{ij} = \frac{\partial P_i}{\partial \varepsilon_j}. \tag{15}$$

As in fact $P_i \equiv P_i^{(b)}$, and taking into account that $V \equiv V(\varepsilon_j)$ and, in general, $\mathbf{R} \equiv \mathbf{R}(\varepsilon_j)$, an infinite number of e_{ij} values can be obtained according to the selected $P_i^{(b)}$ branch. A simple way to bypass this problem, according to Vanderbilt's suggestion,[39] is the following. Let us define the $\phi_l^{(\xi)}$ phase components, projecting $\mathbf{r}_A$ and $\overline{\mathbf{r}}_t$ along the reciprocal-lattice vectors $\mathbf{b}_l$ ($\mathbf{b}_l \cdot \mathbf{a}_i = 2\pi\, \delta_{li}$, where $\mathbf{a}_i$ are primitive-cell vectors),

TABLE III. Characterization of a WF centered on Zn (first entry in Table II) and of the most diffuse one centered on O (type 1 of ZnO system). $q_A^{\mathbf{g}}$ (in $|e|$) is the fraction of the total density of the WF attributed to atom A in cell $\mathbf{g}$ according to a Mulliken partition [Eq. (6)]. $S = \Sigma_{A,\mathbf{g}} q_A^{\mathbf{g}}$ is the sum of the contributions of the actual and previous lines; only contributions larger than $|0.0001||e|$ are reported. The density is normalized to 1.

Atom	A	$\mathbf{g}$	$q_A^{\mathbf{g}}$	A	$\mathbf{g}$	$q_A^{\mathbf{g}}$	A	$\mathbf{g}$	$q_A^{\mathbf{g}}$	S
Zn	Zn_1	(0,0,0)	0.9961							0.9961
	O_2	$(-1,0,0)$	0.0013	O_2	(0,1,0)	0.0013				0.9987
	O_2	(0,0,0)	0.0007	O_1	(0,0,0)	0.0005				0.9999
O	O_1	(0,0,0)	0.9248							0.9248
	Zn_1	$(0,-1,0)$	0.0680							0.9928
	Zn_1	(0,0,0)	0.0028	Zn_1	(1,0,0)	0.0027	Zn_2	(0,0,0)	0.0026	1.0009
	Zn_2	(1,1,0)	0.0001	Zn_2	(0,1,0)	0.0001	O_2	$(0,0,-1)$	-0.0001	
	O_1	(1,1,0)	-0.0001	O_1	(0,1,0)	-0.0001	O_2	$(1,0,-1)$	-0.0001	
	O_2	$(0,-1,-1)$	-0.0002	O_1	$(-1,-1,0)$	-0.0003	O_1	$(0,-1,0)$	-0.0003	
	O_2	$(0,-1,0)$	-0.0003							0.9997

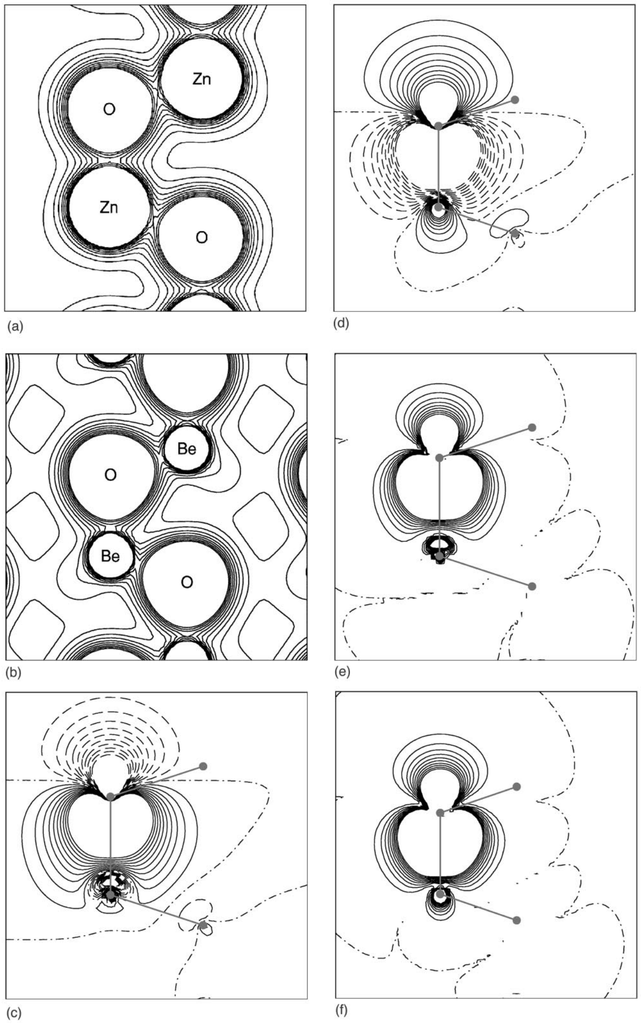

FIG. 1. Total electron-charge-density map (top), Type-1 WF in O (middle), and their associated electron-density maps (bottom) in the (110) plane for ZnO and BeO. Consecutive isodensity lines differ by 0.01 for the top and middle and by 0.001 e/bohr^3 for the bottom pictures. Curves corresponding to absolute values larger than 0.1 (top and middle) and 0.001 e/bohr^3 (bottom) are not plotted. Continuous, dashed, and dot-dashed lines denote positive, negative, and zero values. Gray circles indicate the nuclei positions. Maps are 6.1 Å wide.

$$\phi_l^{(\xi)} = \sum_{A=1}^{P} Z_A \mathbf{b}_l \cdot \mathbf{r}_A^{(\xi)} - \sum_{t=1}^{N} 2\,\mathbf{b}_l \cdot \overline{\mathbf{r}_t}^{(\xi)}. \qquad (16)$$

Note that $\phi_l^{(\xi)}$ is an adimensional quantity. Suppose now vector $\mathbf{R}_p = p_1\mathbf{a}_1 + p_2\mathbf{a}_2 + p_3\mathbf{a}_3$ is added to $\mathbf{r}_A$ or $\overline{\mathbf{r}_t}$; $\phi_l^{(\xi)}$ will now change by a multiple of 2π, which is obviously independent of ε_j. The "proper"[39] piezoelectric constant takes then the form

$$\tilde{e}_{ij} = \frac{1}{2\pi} \frac{e}{V_0} \sum_l \frac{d\phi_l}{d\varepsilon_j} a_{li}, \qquad (17)$$

where the constant term disappears in the derivative with respect to ε_j. It is then convenient to define both the electronic and nuclear contributions with reference to the

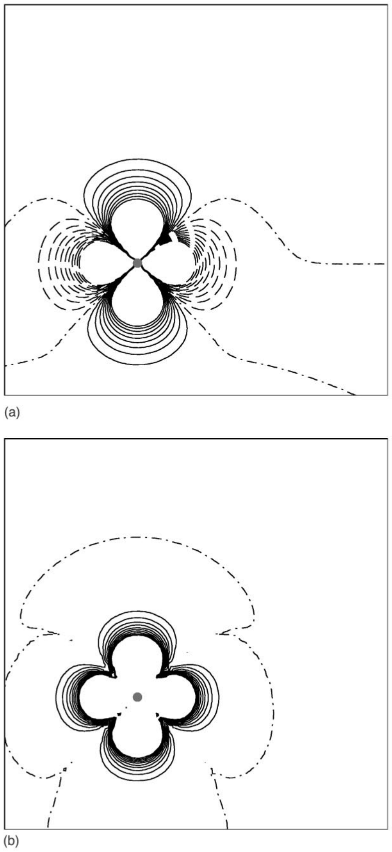

FIG. 2. A *d*-type WF (top) and its square (bottom) centered on Zn. Scale, symbols, and sizes are as in FIG. 1

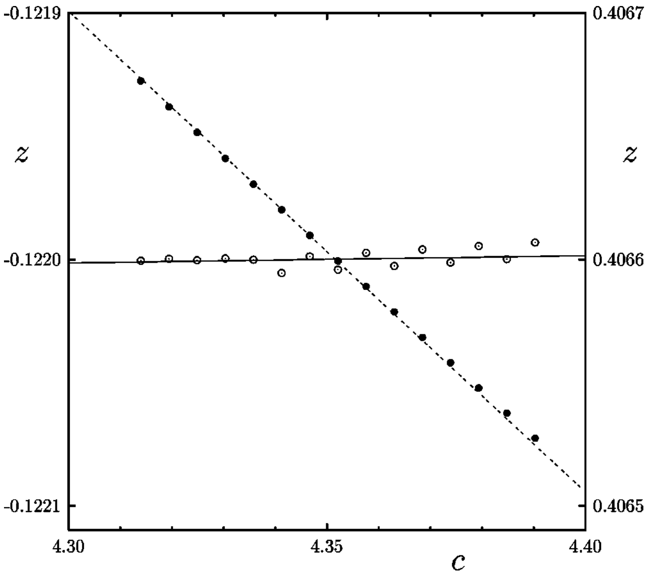

FIG. 3. Dependence of the centroid *z* fractional coordinate for a core (left scale, continous line and open circles) and a valence (right scale, dashed line and full circles) LWF of BeO centered on oxygen, as a function of the cell parameter *c* (in Å). $\partial z/\partial c = 2.0\times10^{-3}$ and 3.0×10^{-5} Å^{-1} for valence and core centroids, respectively.

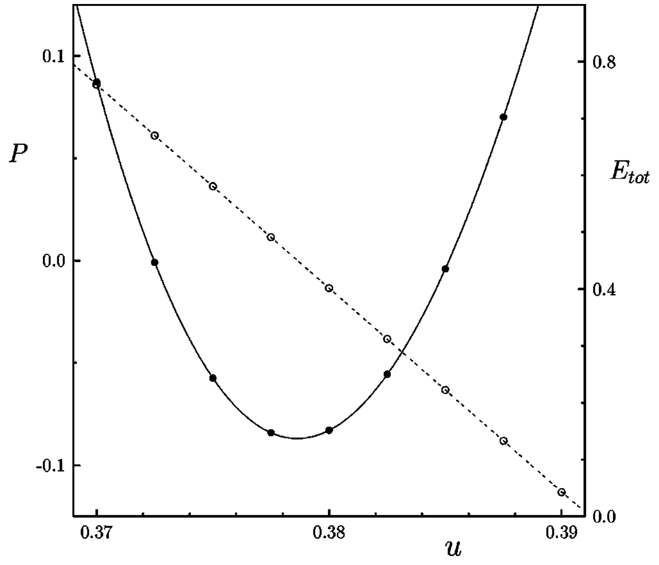

FIG. 4. BeO polarization P in C/m^2 (dashed line and open circles) and energy of the system E_{tot} (solid line and full circles, in mhartree and shifted by -179.4355 hartree) as a function of u, the fractional coordinate of oxygen. $\partial P/\partial u = -9.946$ C/m^2

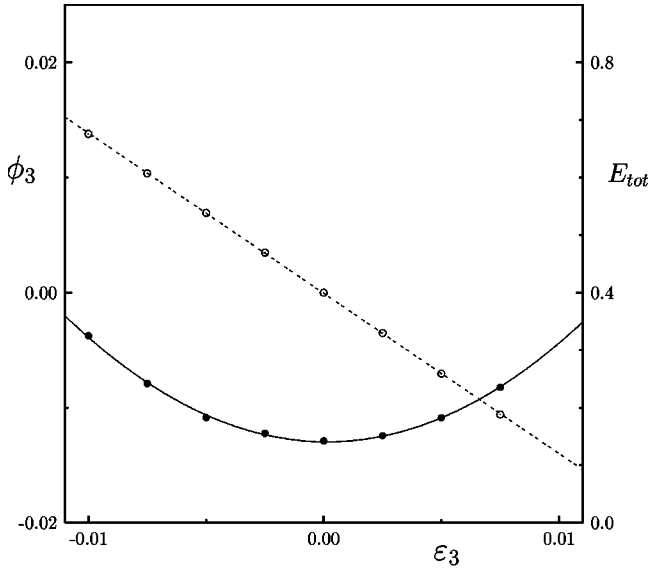

FIG. 5. BeO phase component ϕ_3 (dashed line and open circles) and total energy E_{tot} (solid line and full circles, in mhartree and shifted by -179.4355 hartree) as a function of the strain ε_3. $\partial\phi_3/\partial\varepsilon_3 = -1.393$ corresponding to $\tilde{e}_{33}^{(0)} = -0.569$ C/m^2. See text for more details.

reciprocal-lattice-vector directions according to Eq. (16), and this is the way they are implemented in the CRYSTAL code.

Another quantity that will be used in the following section is the Born, or transverse, dynamical charge tensor Z^*, defined as the coefficient of proportionality at the linear order between the macroscopic polarization per unit cell created in a direction j and a rigid displacement, τ_{i_κ}, of the sublattice of atoms κ in direction i, times the equilibrium unit-cell volume V_0,

$$Z^*_{i_\kappa,j} = V_0 \frac{\partial P_j}{\partial \tau_{i_\kappa}} \qquad (18)$$

C. The Berry-phase approach and piezoelectric calculations

For a periodic insulating crystal, the electronic contribution of the tth band to the BP along the reciprocal-lattice vector $\mathbf{b}_l$ can be written as[39]

$$\phi_{t,l}^{(\xi)} = \frac{1}{V_{BZ}} \int d^3k \langle u_t^{(\xi)}(\mathbf{k}) | -i\mathbf{b}_l \cdot \nabla_{\mathbf{k}} | u_t^{(\xi)}(\mathbf{k}) \rangle, \qquad (19)$$

where V_{BZ} is the first Brillouin-zone volume and $u_t^{(\xi)}(\mathbf{k},\mathbf{r}) = e^{i\mathbf{k}\cdot\mathbf{r}}\psi_t^{(\xi)}(\mathbf{k},\mathbf{r})$, where the BF $\psi_t^{(\xi)}(\mathbf{k})$ [see Eq. (1)] are the eigenvectors of the one-electron ground-state Hamiltonian referring to the nuclear and cell configuration ξ. The nuclear contribution to the phase can be projected along the reciprocal-lattice vectors in the same way as in the LWF formalism, so that the total phase $\phi_l^{(\xi)}$ is in both cases (LWF and BP) the starting point for the calculation of the piezoelectric coefficients.

D. The piezoelectric tensor in the wurtzite structure

In the wurtzite structure (hexagonal Bravais lattice, C_{6v} point group), the unit cell contains four atoms and is fully

TABLE IV. Dependence of the spontaneous polarization ($\mathbf{P}_{eq}$) and piezoelectricity of BeO, evaluated through the BP and the LWF techniques, on the shrinking factor defining the reciprocal-space mesh. The shrinking factor I_S is the same for the three directions ($I_S = I_{S_1} = I_{S_2} = I_{S_3}$). N is the corresponding number of irreducible k points in the first Brillouin zone. t is the computational time (on a Pentium III 800-MHz personal computer). $\tilde{e}_{33}^{(0)}$ is the clamped-ion term of the $\tilde{e}_{33}$ proper piezoelectric tensor component (see text for more details). $\mathbf{P}_{eq}$ and $\tilde{e}_{33}^{(0)}$ in C/m^2.

		BP			LWF		
I_S	N	t	$\mathbf{P}_{eq}$	$\tilde{e}_{33}^{(0)}$	t	$\mathbf{P}_{eq}$	$\tilde{e}_{33}^{(0)}$
2	4	13	-0.036	-0.5597			
3	6	48	-0.036377	-0.5743	9	-0.036278	-0.5579
4	12	119	-0.036350	-0.5748	20	-0.036312	-0.5652
5	15	226	-0.036338	-0.5746	38	-0.036312	-0.5679
6	28	390	-0.036330	-0.5744	65	-0.036306	-0.5698
8	50	1224	-0.036323	-0.5743	120	-0.036308	-0.5710
10	84	1789	-0.036318	-0.5742	188	-0.036308	-0.5709

TABLE V. Proper piezoelectric-tensor components ($\tilde{e}_{ij}$; $\tilde{e}_{ij}^{(0)}$ is the clamped-ion contribution) evaluated through the BP and the LWF schemes. Spontaneous polarization $\mathbf{P}_{eq}$ and $\tilde{e}_{ij}$ in C/m^2. Z^* is the Born effective charge (in e)

		$\mathbf{P}_{eq}$	Z^*	$\tilde{e}_{33}^{(0)}$	$\tilde{e}_{31}^{(0)}$	$\tilde{e}_{33}$	$\tilde{e}_{31}$
BeO	BP	−0.03633	−1.9432	−0.5744	0.2881	0.0364	−0.0735
	LWF	−0.03631	−1.9419	−0.5698	0.2898	0.0399	−0.0715
ZnO	BP	−0.05696	−2.0711	−0.4459	0.2210	1.1998	−0.5336
	LWF	−0.05691	−2.0627	−0.4447	0.2214	1.1943	−0.5300

defined by the length of the hexagonal edge a_0, the height c_0 of the prism [so the equilibrium cell volume is $V_0 = (\sqrt{3}/2)a_0^2 c_0$], and u, the fractional z coordinate of the oxygen sublattice. Both the cations and anions are tetrahedrally coordinated. The piezoelectric tensor has just three independent components.[40] Two of them measure the polarization induced along the c axis, at zero electric field, by a uniform strain either along the c axis or in the basal plane. The third component describes the polarization induced perpendicularly to the c axis by a shear strain; as it implies a large symmetry reduction and a time-consuming ionic relaxation, it will not be considered in the present work. Equation (14) then becomes in the present case

$$P_3 = e_{33}\varepsilon_3 + e_{31}(\varepsilon_1 + \varepsilon_2), \tag{20}$$

where $\varepsilon_3 = (c - c_0)/c_0$ and $\varepsilon_1 = \varepsilon_2 = (a - a_0)/a_0$.

Conventionally, the sign of the piezoelectric-tensor components is fixed by assuming that the positive direction along the c axis goes from the cation to the anion.

Equation (20) is a macroscopic phenomenological equation describing, in the linear regime, the piezoelectric-tensor components in terms of a change of the polarization $\mathbf{P}$ induced by a variation of the cell parameters a and c. Microscopically, a strain ε_j produces also, in general, an internal displacement of one sublattice with respect to the other. In our case that is a variation of the $z_{O_1} = cu$ and $z_{O_2} = c(u - \frac{1}{2})$ coordinates. We then separate the two contributions as follows, in deriving e_{33} from Eq. (20):

$$e_{33} = \left.\frac{\partial P_3}{\partial \varepsilon_3}\right|_u + \left.\frac{\partial P_3}{\partial u}\right|_{\varepsilon_3} \frac{du}{d\varepsilon_3}. \tag{21}$$

The first term (the *clamped-ion* term,[41,24] usually indicated as $e_{33}^{(0)}$) gives the effect of the modification of the cell parameters at fixed fractional coordinates. The second term, which gives the effect of the u relaxation, is usually defined in terms of the components of the Born dynamical charge tensor Z^* which is defined in Eq. (18),

$$Z^*_{z_O,3} \equiv Z^* = \frac{\sqrt{3}}{2} a_0^2 c_0 \frac{\partial P_3}{\partial (z_{O_1} + z_{O_2})} \tag{22}$$

$$= \frac{\sqrt{3}a_0^2}{4} \frac{\partial P_3}{\partial u}. \tag{23}$$

Equation (21) then becomes

$$e_{33} = e_{33}^{(0)} + k\, Z^* \frac{du}{d\varepsilon_3}, \tag{24}$$

where $k = 4/\sqrt{3}a_0^2$. In a similar way

$$e_{31} = e_{31}^{(0)} + k\, Z^* \frac{du}{d(\varepsilon_1 + \varepsilon_2)}, \tag{25}$$

where

$$e_{31}^{(0)} = \left.\frac{\partial P_3}{\partial (\varepsilon_1 + \varepsilon_2)}\right|_u. \tag{26}$$

In order to avoid the multivalued problem (see discussion in Sec. II B 2), the clamped-ion terms are actually evaluated according to Eq. (17),

$$\tilde{e}_{33}^{(0)} = \frac{1}{2\pi} \frac{e}{V_0} \sum_l \left.\frac{d\phi_l}{d\varepsilon_3}\right|_u a_{l3}, \tag{27}$$

a_{13} and a_{23} are zero (the c axis coincides with the z cartesian axis), so Eq. (27) takes a very simple form,

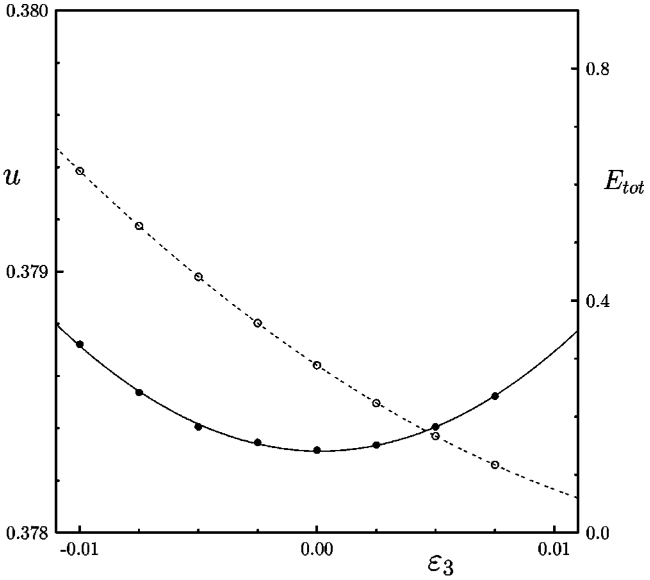

FIG. 6. Equilibrium fractional coordinate of oxygen u (dashed line and open circles) and energy of the system E_{tot} (solid line and full circles, in mhartree and shifted by −179.435 hartree) as a function of the strain ε_3.

TABLE VI. Comparison of BeO and ZnO piezoelectric constants calculated through the LWF scheme with previous calculations (Refs. 38 and 41) and experiments (Refs. 44 and 45). $\mathbf{P}_{eq}$ is the spontaneous polarization in C/m^2. Z^* is the Born effective charge (in e); other entries are contributions to the piezoelectric constants (in C/m^2); see text for more details.

		$\mathbf{P}_{eq}$	Z^*	$du/d\varepsilon_3$	$du/d(\varepsilon_1+\varepsilon_2)$	$e_{33}^{(0)}$	$e_{31}^{(0)}$	e_{33}	e_{31}
BeO	Our work	-0.036	-1.94	-0.061	0.036	-0.57	0.29	0.04	-0.07
	Ref. 41	-0.05	-1.72	-0.09		0.29		0.50	
	Ref. 38	-0.045	-1.85	-0.06		-0.60	0.35	0.02	-0.02
	Expt.		-1.85 [a]					0.10 [b]	
ZnO	Our work	-0.057	-2.06	-0.23	0.11	-0.44	0.22	1.19	-0.53
	Ref. 41	-0.05	-2.05	-0.25		-0.58	0.37	1.21	-0.51
	Ref. 38	-0.057	-2.11	-0.21		-0.66	0.38	0.89	-0.51
	Expt.		-2.10 [a]					1.00–1.55 [b]	

[a] Reference 44.

[b] Reference 45.

$$\tilde{e}_{33}^{(0)}=\frac{a_{33}e}{2\pi V_0}\left.\frac{d\phi_3}{d\varepsilon_3}\right|_u . \tag{28}$$

The other clamped-ion component $\tilde{e}_{31}^{(0)}$ is evaluated in the same way,

$$\tilde{e}_{31}^{(0)}=\frac{a_{33}e}{2\pi V_0}\left.\frac{d\phi_3}{d\varepsilon_1}\right|_u=\frac{a_{33}e}{\pi V_0}\left.\frac{d\phi_3}{d(\varepsilon_1+\varepsilon_2)}\right|_u . \tag{29}$$

III. RESULTS AND DISCUSSION

The main features of the ZnO and BeO WF's are summarized in Table II. The BeO situation is very simple; there are four nearly equivalent valence WF's, localized on O (the centroid being at about 0.37 Å from the atom) with a localization index very close to 1, confirming the fully ionic nature of this compound. The four valence WF's of ZnO are at about the same distance from O as they are in the BeO case; however, they are slightly more diffuse (see the σ column in Table II) with a higher delocalization index λ, indicating some degree of participation of the Zn atom. This is confirmed by Table III, where the WF's are analyzed in terms of a Mulliken analysis: the population on the oxygen atom on which the WF is located is 0.92e; about 0.08 electrons are on the nearest Zn ions, and only populations smaller than 0.0004e can be found on the second and farther neighbors. The degree of localization of the oxygen WF's in the two systems is better appreciated from Fig. 1, where both the WF and its square are reported. The d WF's are even more localized, and maintain to a large amount the atomic character, as shown by the two tables (II and III) and the figure showing one of these WF's (Fig. 2).

It is interesting to investigate how $\overline{\mathbf{r}}_t$, the WF centroid, moves as a function of the strain. Let us consider, for example, $e_{33}^{(0)}$, the "clamped-ion" contribution to e_{33}. If the centroid follows rigidly the atom to which the WF "belongs," the displacement of the electronic charge due to the strain would exactly be canceled by the same (in modulus) and opposite (in sign) displacement of a fraction of the nuclear charge, and the net effect would be zero. This is the case of the core WF's, which move very rigidly with the nucleus, as shown in Fig. 3, where the continuous line refers to the 1s WF of oxygen in BeO (the fractional z coordinate of the centroid does not change when the c axis is contracted or expanded). The dashed line, on the contrary, referring to one of the four valence WF's of BeO, is far from being horizontal, and generates a net contribution to the piezoelectric constant (see Table VI).

According to Eq. (15), the calculation of e_{33} and e_{31} requires the estimate of three numerical derivatives, namely (in the e_{33} case), $Z^*=kdP_3/du$, $e_{33}^0=|\partial P_3/\partial\varepsilon_3|_u$, and $du/d\varepsilon_3$. A question can be raised, then, concerning the accuracy that can be attained with a particular computer code (CRYSTAL98 in the present case) in the numerical evaluation of these derivatives, and how the error propagates to the final value of e_{33} and e_{31}; it is interesting to notice that the first two derivatives are evaluated according to different algorithms, when the WF or the BP schemes are adopted; a good agreement between the values obtained with BP and WF for Z^* and e_{33}^0 would represent a strong, although indirect, evidence of the high numerical accuracy of the two schemes. Figures 4 and 5 provide the dependence of P_3 on u, and on ε_3 in a relatively small interval around the equilibrium geometry. In both cases, the evaluated points (obtained from the WF centroids) show an extremely good linear behavior, indicating that the numerical noise is very small.

In Table IV the dependence of the spontaneous polarization $\mathbf{P}_{eq}$ and of the $e_{31}^{(0)}$ contribution to the piezoelectric constant on the shrinking factor I_S adopted for the two algorithms (BP and LWF) is reported. It turns out that in both cases convergence is quite rapid, and that beyond $I_S=5$ both quantities change by less than 0.1%.

In Table V the values obtained for the two systems with LWF are compared with the corresponding values obtained with the BP scheme: it turns out that they are extremely similar, the differences being always much smaller than 1%. Also the spontaneous polarization $\mathbf{P}_{eq}$ (see Ref. 41 for the definition of the reference geometries to be used for $\mathbf{P}_{eq}$, and its meaning in the case of the wurtzite geometry) obtained with the two methods are very close to each other.

The last numerical derivative to be evaluated, $du/d\varepsilon_3$, is obviously common to the two techniques and is probably the most delicate, because the *u* points appearing in Fig. 6 are the results of a preliminary optimization (the best *u* value for a given ε_3). As $du/d\varepsilon_3$ is multiplied by the Born charge, which is a relatively large number, small inaccuracies in $du/d\varepsilon_3$ can result in relatively large error bars in the total piezoelectric constant, also because the two contributions (the clamped-ion term and the one we are talking about) do have opposite signs and tend to cancel each other. Figure 6 shows that also in the relatively small interval explored here (the spanned energy interval is just a fraction of a mHartree) *u* is not a linear function of ε_3; in the present case a parabolic interpolation has been used, and the coefficient of the linear term has been inserted in Eq. (21).

In Table VI the present results are compared with previous calculations by Dal Corso *et al.*[41] and Bernardini *et al.*,[38] and with the few available experimental results. It must be underlined that in the present study we used an all-electron basis set and the HF Hamiltonian; in the case of Dal Corso *et al.*, the local-density-approximation Hamiltonian has been used with a FLAPW-type scheme; Bernardini *et al.*, finally, used a plane-waves code, ultrasoft pseudopotentials, and a generalized-gradient-approximation Hamiltonian. A quite good agreement is observed with Bernardini *et al.* in the BeO case, both for the total e_{ij} and for the various terms contributing to them. The largest absolute difference between our calculations and those of Bernardini *et al.* (0.05 C/m^2) is then extremely small. Both calculations are quite close to the only experimental available datum referring to e_{33}. e_{33} obtained by Dal Corso *et al.* is higher than the present one by 0.46 C/m^2 (and by 0.40 C/m^2 than experiment), as a result of relatively large differences in all contributions ($\mathbf{Z}^*, du/d\varepsilon_3, e_{33}^{(0)}$). As regards ZnO, the three calculations agree quite well for e_{31} (note, however, that this agreement is the result of the cancellation of relatively large differences in the partial contributions, as shown by $e_{31}^{(0)}$ and Z^* data). For e_{33}, on the contrary, the present data are very close to the results of Dal Corso *et al.* and fall in the (relatively large) experimental interval. The data of Bernardini *et al.* are 0.3 C/m^2 smaller than the present ones, and below the lowest experimental determination.

The point concerning the influence on the set of properties investigated here of the adopted Hamiltonian, basis set, and all the specific features connected to the implementation of the computational scheme in a given computer program deserves then additional investigation, as such a kind of analysis is at the moment scarce and not systematic in the literature.

In summary, in the present paper it has been shown that delicate quantities such as the spontaneous polarization and its derivatives can be calculated in a straighforward and intuitive way starting from very-well-localized WF and using a HF Hamiltonian and a localized basis set; the results are fully equivalent to the ones obtained through a Berry-phase scheme (when the same basis set and Hamiltonian is used), and agree quite well with the available experimental results.

ACKNOWLEDGMENTS

R.D. thanks the P. & M. Curie University for a short period grant. C.M.Z.-W. and Y.N. thank the University of Torino for a grant.

---

[*] Permanent address: Departamento de Física, Universidad Autónoma del Estado de Morelos, Av. Universidad 1001, Col. Chamilpa, 62210 Cuernavaca (Morelos), Mexico.

[†] Author to whom correspondence should be addressed. Email address: dovesi@ch.unito.it

[1] N. Marzari and D. Vanderbilt, Phys. Rev. B **56**, 12 847 (1997).
[2] M. Klessinger, Int. J. Quantum Chem. **23**, 535 (1983).
[3] A. Julg, Int. J. Quantum Chem. **26**, 709 (1984).
[4] A.E. Reed and F. Weinhold, J. Chem. Phys. **83**, 1736 (1985).
[5] P. Nagy, J.G. Ángyán, G. Náray-Szabó, and G. Peinel, Int. J. Quantum Chem. **31**, 927 (1987).
[6] P.R. Surján, J. Pipek, and B. Paizs, Theor. Chim. Acta **86**, 379 (1993).
[7] J. Pipek and I. Varga, Phys. Rev. A **46**, 3148 (1992).
[8] C.J. Calzado, J.-P. Malrieu, and J.F. Sanz, J. Phys. Chem. **102**, 3659 (1998).
[9] S. Diner, J.P. Malrieu, P. Claverie, and F. Jordan, Chem. Phys. Lett. **2**, 319 (1968).
[10] P. Otto and J. Ladik, Int. J. Quantum Chem. **22**, 169 (1982).
[11] E. Kapuy, Z. Csépes, and C. Kozmutza, Int. J. Quantum Chem. **23**, 981 (1983).
[12] P. Pulay, Chem. Phys. Lett. **100**, 151 (1983).
[13] M. Haser and J. Almlöf, J. Chem. Phys. **96**, 489 (1991).
[14] M. Schütz, G. Hetzer, and H.-J. Werner, J. Chem. Phys. **111**, 5691 (1999).
[15] S. Koch and W. Kutzelnigg, Theor. Chim. Acta **59**, 387 (1981).
[16] W. Kutzelnigg, in *Localization and Delocalization in Chemistry*, Atoms and Molecules in the Ground State Vol. 1, edited by O. Chalvet, R. Daudel, S. Diner, and J. P. Malrieu (Reidel, Dordrecht, 1975), pp. 143–153.
[17] M.F. Guest and V.R. Saunders, Mol. Phys. **35**, 575 (1978).
[18] S. Saebø, Int. J. Quantum Chem. **38**, 641 (1990).
[19] C. Hampel and H.-J. Werner, J. Chem. Phys. **104**, 6286 (1996).
[20] P. J. Knowles, M. Schütz, and H.-J. Werner, in *Modern Methods and Algorithms in Quantum Chemistry*, 2nd ed., edited by J. Grotendorst (NIC Series, Jülich, 2000), Vol. 3.
[21] M. Schütz and H.-J. Werner, J. Chem. Phys. **114**, 661 (2001).
[22] R. Pick, M. Cohen, and R. Martin, Phys. Rev. B **1**, 910 (1970).
[23] P. Ghosez, J. Michenaud, and X. Gonze, Phys. Rev. B **58**, 6224 (1998).
[24] R. King-Smith and D. Vanderbilt, Phys. Rev. B **47**, 1651 (1993).
[25] R. Resta, Ferroelectrics **136**, 51 (1992).
[26] R. Resta, Europhys. Lett. **22**, 133 (1993).
[27] R. Resta, Rev. Mod. Phys. **66**, 899 (1994).
[28] C. M. Zicovich-Wilson, R. Dovesi, and V. R. Saunders, J. Chem. Phys. (to be published).
[29] S. Dall'Olio, R. Dovesi, and R. Resta, Phys. Rev. B **56**, 10 105 (1997).
[30] V. Saunders, R. Dovesi, C. Roetti, M. Causa, N. Harrison, R. Orlando, and C. M. Zicovich-Wilson, CRYSTAL98 *User's Manual*,

Università di Torino, Torino, 1998.

[31] J. Jaffe, N. Harrison, and A. Hess, Phys. Rev. B **49**, 11 153 (1994).

[32] Basis sets are available at the following web site: http://www.ch.unito.it/ifm/teorica/Basis_Sets/mendel.html.

[33] A. Lichanot, M. Chaillet, C. Larrieu, R. Dovesi, and C. Pisani, Chem. Phys. Lett. **164**, 383 (1992).

[34] H. Monkhorst and J. Pack, Phys. Rev. B **13**, 5188 (1976).

[35] S. Boys, Rev. Mod. Phys. **32**, 296 (1960).

[36] J. Foster and S. Boys, Rev. Mod. Phys. **32**, 300 (1960).

[37] Ph. Baranek, C. M. Zicovich-Wilson, C. Roetti, R. Dovesi, and V. Saunders, Phys. Rev. B **64**, 125102 (2001).

[38] F. Bernardini, V. Fiorentini, and D. Vanderbilt, Phys. Rev. B **56**, R10 024 (1997).

[39] D. Vanderbilt, J. Phys. Chem. Solids **61**, 147 (2000).

[40] J. Nye, *Physical Properties of Crystals: Their Representation by Tensors and Matrices* (Oxford Univ Press, London, 1987).

[41] A. Dal Corso, M. Postenak, R. Resta, and A. Baldereschi, Phys. Rev. B **50**, 10 715 (1994).

[42] R.M. Hazen and L.W. Finger, J. Appl. Phys. **59**, 3728 (1986).

[43] O. Madelung, M. Schultz, and H. Weiss, *Numerical Data and Functional and Relationships in Science and Technology* (Springer-Verlag, Berlin, 1982), Vol. 17.

[44] R.M. Martin, Phys. Rev. B **5**, 1607 (1972).

[45] O. Madelung, W. von der Osten, and U. Rössler, in *Zahlenwerte und Funktionen aus Naturwissenshaften und Technik*, edited by O. Madelung and M. Schultz, Landolt-Börnstein, New series, Group III, Vol. 22, Pt. a (Springer-Verlag, Berlin, 1987), p. 164; *ibid.*, Vol. 17, Pt. b, pp. 342 and 376; *ibid.*, Vol. 11, p. 370.